



Encapsulation of Urea–Ammonium Nitrate (UAN) Solution Fertilizer in Silica–Cellulose Matrix for Slow–Release Nitrogen and Improved Growth of Pakcoy (*Brassica rapa L.*)

Rizki Permata Sari, Choiril Azmiyawati*, Sriatun

Chemistry Department, Faculty of Sciences and Mathematics, Diponegoro University, Semarang, Indonesia

* Corresponding author: choiril.azmiyawati@lecturer.undip.ac.id

<https://doi.org/10.14710/jksa.29.2.73-81>

Article Info

Article history:

Received: 29th November 2025

Revised: 29th January 2026

Accepted: 03rd February 2026

Online: 14th March 2026

Keywords:

mesoporous silica; cellulose; UAN fertilizer; encapsulation; slow-release fertilizer

Abstract

Nitrogen (N) is an essential macronutrient required for plant growth; however, its absorption efficiency remains relatively low due to significant nitrogen loss to the environment. To overcome this limitation, the development of slow-release fertilizers (SRF) is crucial, enabling controlled, gradual nutrient release. This study aims to develop and evaluate a cellulose-modified mesoporous silica matrix as an encapsulation material for Urea–Ammonium Nitrate (UAN) fertilizer, a liquid formulation containing urea, ammonium, and nitrate. The material was synthesized using the sol-gel method with variations including pure silica, non-calcined silica–cellulose, silica–cellulose calcined at 550°C and 700°C, and cross-linking with glutaraldehyde. Characterization techniques included Fourier Transform Infrared Spectroscopy (FTIR) for functional group identification, Scanning Electron Microscopy combined with Energy Dispersive X-ray (SEM-EDX) for morphology and elemental composition, and Gas Sorption Analyzer (GSA) for surface area and pore size analysis. The results showed that the silica–cellulose composite calcined at 550°C (SSCGK550) had the highest fertilizer release value of 893.7 ppm. Plant growth test results show that plants treated with SSCGK550 had the highest growth, with a length of 8 cm and 8 leaves per stem by day 15, whereas plants treated with conventional fertilizer (control) showed a lower growth response, with an average height of 5 cm and only 3 leaves per stem by day 15. These findings demonstrate the success of encapsulating UAN fertilizer in a silica–cellulose matrix and highlight its potential as an efficient slow-release fertilizer to support sustainable agriculture.

1. Introduction

Fertilizers and water play a crucial role in modern agricultural production, making it essential to improve the efficient use of these resources. However, most fertilizers contribute to environmental pollution and health problems due to water eutrophication. The use of conventional fertilizers often results in nutrient concentrations that are excessively high for effective plant uptake. Such high concentrations can lead to undesirable side effects both in the target area and the surrounding environment, potentially causing plant damage and ecosystem disruption [1].

Nitrogen (N) is one of the essential macronutrients required for plant growth. It plays a vital role in the

formation of chlorophyll, proteins, and other organic compounds that support the vegetative development of plants [2, 3]. Nitrogen requirements can be met through fertilizers, including urea. However, urea has several disadvantages, including its potential to degrade soil quality with excessive or prolonged use. Moreover, urea is a fast-release fertilizer, leading to low efficiency and limited nitrogen uptake by plants. Therefore, it is necessary to develop modifications that can control the release of urea [4].

A common approach to reducing nitrogen losses is the development of slow-release fertilizers (SRF). The primary objective of SRF is to maintain an optimal nutrient concentration in the soil, thereby reducing

fertilization costs and frequency while allowing nutrients to be gradually released into the soil to improve fertilizer efficiency [5]. The UAN fertilizer (a liquid formulation containing urea, ammonium, and nitrate) modified through the SRF method has emerged as an alternative liquid fertilizer that delivers nitrogen in three forms: nitrate, ammonium, and amide.

In the development of SRF, selecting an appropriate carrier material is a key factor in determining the success of the nutrient slow-release system. An ideal matrix should be capable of effectively adsorbing fertilizers such as urea and ammonium nitrate, while releasing them gradually according to the plant's nutrient requirements [6]. Mesoporous silica has been extensively developed for various adsorption applications due to its tunable particle size, pore size, pore volume, and mesostructure, which can be tailored to specific applications, thereby enabling its optimal utilization. Several applications of mesoporous silica include catalysis, adsorption, molecular separation, drug delivery systems, chemosensors, and biosensors [7].

Over the past decade, SRF has been widely used as an alternative to repeated fertilization for pakcoy crops. In pakcoy crops, the use of SRF has been shown to increase soil nutrient content, soil nitrogen availability, and root development [8]. To enhance the efficiency of mesoporous silica in controlling nutrient release, modifications can be made using polymeric materials, such as cellulose. Cellulose-based polymers can also be used for the adsorption of fertilizers due to their ability to alter silica porosity, regulate nutrient release, and act as pore-forming agents to produce silica particles with tunable size and structure, features that are crucial for microcapsule formation. The advantages of cellulose include its low cost and environmental friendliness, as it is biodegradable. Furthermore, cellulose exhibits excellent coating properties, allowing it to protect various chemical substances from degradation and loss before use. It also possesses superior water-retention capacity, slow-release behavior, and material biodegradability [9].

Reaction temperature is one of the key parameters in the synthesis of silica-cellulose composite materials. Variations in temperature can influence particle size, surface area, structural stability, and the adsorption capacity of the material toward fertilizers. Selecting an appropriate synthesis temperature is expected to enhance the encapsulation efficiency of UAN fertilizer within the composite matrix and to regulate its release rate optimally into the growth medium. Previous studies have reported the use of various silica- and cellulose-based materials as slow-release systems for fertilizers; however, challenges remain, including high production costs, low adsorption efficiency, and excessively slow nutrient release rates [10].

This study combines mesoporous silica and cellulose to form a hybrid matrix specifically designed to encapsulate UAN liquid fertilizer containing urea, ammonium, and nitrate. The effects of synthesis temperature and glutaraldehyde crosslinking on encapsulation efficiency and nitrogen release behavior

were systematically evaluated. This approach provides an inexpensive, biodegradable, and customizable slow-release fertilizer system that has not been reported previously for UAN applications.

2. Experimental

2.1. Materials

The equipment used in this research included standard laboratory glassware and porcelain apparatus, an electric oven (Memmert UN30, Germany), high-temperature furnace (Vulcan 3-130, USA), magnetic stirrer with hot plate (IKA C-MAG HS 7, Germany), analytical balance (Ohaus PA214, USA), desiccator, vacuum filtration apparatus (Büchner funnel and vacuum pump), pH meter (Hanna HI2211, Romania), Fourier Transform Infrared spectrometer (Perkin Elmer Spectrum IR, USA), gas sorption analyzer (Quantachrome ASIQwin 3.01, USA), and scanning electron microscope with EDX (Hitachi SU3500, Japan). The materials included technical-grade sodium silicate (Na_2SiO_3) (Brataco, Indonesia), carboxymethyl cellulose (Sigma-Aldrich, Germany), 37% hydrochloric acid (Merck, Germany), 25% glutaraldehyde (Merck, Germany), UAN liquid fertilizer (self-prepared urea-ammonium nitrate formulation), and distilled water.

2.2. Methods

2.2.1. Synthesis of Cellulose-Modified Mesoporous Silica

A total of 18.006 g of CMC was gradually dissolved in 690 mL of deionized water under heating and stirring at 80°C until a homogeneous solution was obtained. Separately, a Na_2SiO_3 solution was prepared by dissolving 90 mL of Na_2SiO_3 in 120 mL of deionized water (10% w/v). This solution was then added to the CMC solution and stirred for 30 minutes. Subsequently, 3 M HCl was added dropwise until the pH of the mixture reached 6–7. The mixture was maintained at 80°C under continuous stirring for 4 hours, then cooled to room temperature and stirred for an additional 24 hours.

2.2.2. Separation and Drying of Cellulose-Modified Mesoporous Silica

The resulting mixture was filtered and washed thoroughly with deionized water. The solid product was dried in an oven at 105°C, then ground in a mortar and pestle to obtain a fine powder. The sample was divided into two portions: one was kept as the non-calcined sample (SSCGNK), while the other was calcined at 550°C (SSCGK550) and 700°C (SSCGK700) with a heating rate of 5°C/min for 6 hours to obtain a white powder [11].

2.2.3. Adsorption of UAN Fertilizer into Silica Matrix (SRF-M Method)

The mesoporous silica was classified into four types: pure silica (SCG), cellulose-modified non-calcined silica (SSCGNK), and cellulose-modified silica calcined at 550°C (SSCGK550) and 700°C (SSCGK700). Each type of silica was mixed with UAN fertilizer at a 1:4 (w/v) ratio in a closed container and allowed to soak for 24 hours to ensure UAN adsorption into the silica matrix.

2.2.4. **Drying of Adsorbed Samples**

The samples were filtered to remove unadsorbed UAN fertilizer and placed in a desiccator for 48 hours to allow complete evaporation of any fertilizer remaining on the silica surface.

2.2.5. **Sample Crosslinking with Glutaraldehyde**

Two grams of each sample were immersed in 12 mL of glutaraldehyde solution and left to stand for 24 hours. The samples were then filtered and dried in a desiccator until a whitish-yellow powder was obtained.

2.2.6. **Sample Characterization**

FTIR (Fourier Transform Infrared Spectroscopy): Samples were mixed with KBr, pressed into thin pellets, and analyzed in the wavenumber range of 400–4000 cm⁻¹ to identify functional groups. SEM-EDX (Scanning Electron Microscope–Energy Dispersive X-ray): Samples were fixed and dried, then observed at 5100× magnification and 5 kV accelerating voltage to examine surface morphology and elemental composition. GSA (Gas Sorption Analyzer): Samples were analyzed using the BET method at liquid nitrogen temperature (77.035 K) and a relative pressure range (P/P₀) of 0.05–0.995 to determine specific surface area, pore volume, and pore-size distribution.

3. **Results and Discussion**

3.1. **Synthesis of Silica**

Silica was synthesized via the sol–gel method under acidic conditions by adding HCl to a sodium silicate solution. The acidification step induced gelation through the formation of silicic acid species, resulting in a white hydrogel. The gel was then aged and repeatedly washed to remove residual salts and impurities. After oven drying, a white xerogel powder was obtained, yielding 2.903 g (Figure 1). The appearance of a white silica powder indicates successful formation of the Si–O–Si network structure. Although the reaction was initiated under acidic conditions, the sol–gel process proceeded optimally as the system approached near-neutral pH during gel maturation. The overall reaction mechanism for silica formation is presented in Equation (1).

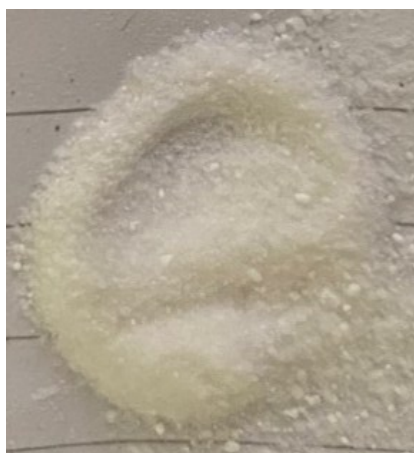
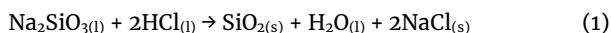


Figure 1. Synthesized silica

3.2. **Synthesis of Cellulose–Modified Silica**

Cellulose–modified silica was synthesized from a mixture of sodium silicate and CMC solution, producing a white powder. The formation of white powder indicated the successful synthesis of silica bonded with CMC. CMC acted as a stabilizing and binding agent during the polymerization process. The hydroxyl (–OH) and carboxyl (–COOH) groups in CMC formed hydrogen and covalent bonds with the silanol (–Si–OH) groups of silica, resulting in Si–O–Si and Si–O–C linkages. Polymerization was conducted for 30 minutes under stirring, followed by acidification with 3 M HCl to pH ~7, yielding a light-yellow gel. The gel was aged for 24 hours, then dried and ground into fine powder. The reaction scheme is shown in Figure 2.

The hydroxyl groups of cellulose initially interact with Si–OH groups through hydrogen bonding, facilitating the distribution of silica precursors along the polymer chains and promoting nucleation within the macromolecular network. Subsequently, the silanol groups formed during hydrolysis undergo condensation reactions to generate Si–O–Si linkages, leading to the development of the silica framework. The carbonyl and hydroxyl groups of CMC also react with silanol groups to form covalent Si–O–C bonds, strengthening the organic–inorganic interface [12, 13].

3.3. **Synthesis of Silica Composite for UAN Fertilizer Adsorption**

Silica composites for UAN fertilizer adsorption were prepared by the immersion method (Solvent Retention Film, SRF–M) using four samples: SCG, SSCGNK, SSCGK550, and SSCGK700. Each sample was immersed in UAN solution until white agglomerated granules formed, indicating adsorption into the porous matrix. The granules were then treated with glutaraldehyde to induce crosslinking and partially seal the pores. After coating, a yellowish powder was obtained (Figure 3). The color change from white to yellow indicates the presence of glutaraldehyde in the composite. This modification is expected to reduce pore accessibility and improve nitrogen retention, supporting controlled-release behavior. These results confirm successful incorporation of UAN fertilizer into both pure and cellulose–modified silica matrices.

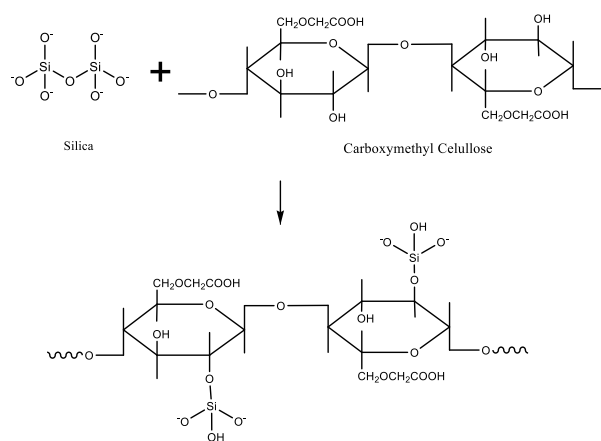


Figure 2. Reaction of carboxymethyl and sodium silicate



Figure 3. Synthesized silica: a) SCG, b) SSCGNK, c) SSCGK550, and d) SSCGK700

3.4. Characterization

3.4.1. FTIR

The FTIR spectra (Figure 4) and the summarized characteristic bands (Table 1) reveal several functional groups in the synthesized silica materials. In SCG, the absorption band at 3220 cm^{-1} corresponds to the stretching vibration of hydroxyl (–OH) groups from surface silanol (Si–OH), confirming the presence of hydroxylated silica surfaces. In SSCGNK, broad absorption bands at 3358–3386 cm^{-1} are attributed to –OH stretching vibrations, indicating contributions from both silanol groups and cellulose-based hydroxyl groups. The bands observed at 1560 cm^{-1} and 1442 cm^{-1} are assigned to the asymmetric and symmetric stretching vibrations of carboxylate (–COO⁻) groups, respectively, originating from CMC, confirming successful incorporation of the organic component into the silica matrix.

After calcination at 550°C, the FTIR spectrum of SSCGK550 exhibits a strong absorption band at 1082 cm^{-1} , corresponding to the asymmetric stretching vibration of Si–O–Si. This band is consistently observed in all samples, including SSCGK700, with slight shifts in the range of 1077–1084 cm^{-1} , indicating minor structural rearrangements due to thermal treatment. The symmetric stretching vibration of Si–O–Si appears at 798–800 cm^{-1} , while the bending vibration is detected at 461–466 cm^{-1} across all samples. The persistence of these characteristic Si–O–Si bands demonstrates that the fundamental silica network structure remains intact despite calcination and glutaraldehyde modification.

The appearance of a new absorption band around 1700 cm^{-1} in SSCGNK is attributed to the stretching vibration of carbonyl (C=O) groups originating from glutaraldehyde, indicating successful surface modification. In addition, absorption bands in the range of 1550–1650 cm^{-1} may be associated with N–H bending vibrations or amide-related modes, likely contributed by nitrogen-containing species from the encapsulated UAN fertilizer (urea and ammonium nitrate).

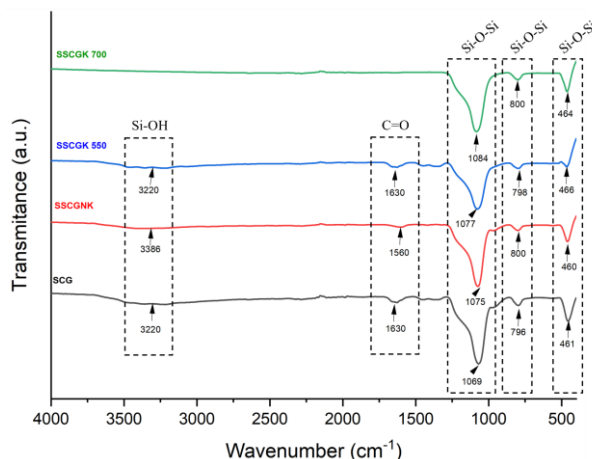


Figure 4. FTIR spectra of SCG, SSCGNK, SSCGK550, and SSCGK700

Table 1. Characteristic FTIR absorption bands of SCG and modified silica samples

Sample	Wavenumber (cm^{-1})		
	Si–OH	C=O	Si–O–Si
SCG	3346	-	461
SSCGNK	3386	1560	460
SSCGK500	3220	1630	466
SSCGK700	2287	-	464

The bands observed at 2850–2950 cm^{-1} correspond to symmetric and asymmetric –CH₂– stretching vibrations of aliphatic groups, which become more prominent in samples modified with glutaraldehyde and loaded with UAN fertilizer. These features collectively suggest the incorporation of organic components within the silica matrix. Shifts in characteristic absorption wavenumbers in SSCGNK, particularly in the –OH region (~3220 cm^{-1}) and other functional group regions (e.g., ~1349 cm^{-1}), indicate changes in the chemical environment due to glutaraldehyde crosslinking and/or thermal treatment. Variations in band intensity further support interactions between glutaraldehyde and surface silanol groups, leading to structural modification of the silica framework.

3.4.2. GSA

GSA characterization was conducted to evaluate the textural properties of the synthesized materials, including pore size, pore volume, and specific surface area. The analyzed samples consisted of SCG, SSCGNK, and SSCGK550, and SSCGK700. The nitrogen adsorption–desorption isotherms are presented in Figure 5. Based on the isotherm profiles, SCG and SSCGNK exhibit Type IV isotherms with H1 hysteresis loops according to the IUPAC classification. This behavior is characteristic of mesoporous materials and indicates capillary condensation within relatively uniform cylindrical pores, along with multilayer adsorption. The presence of a well-defined hysteresis loop suggests an ordered mesoporous structure [11].

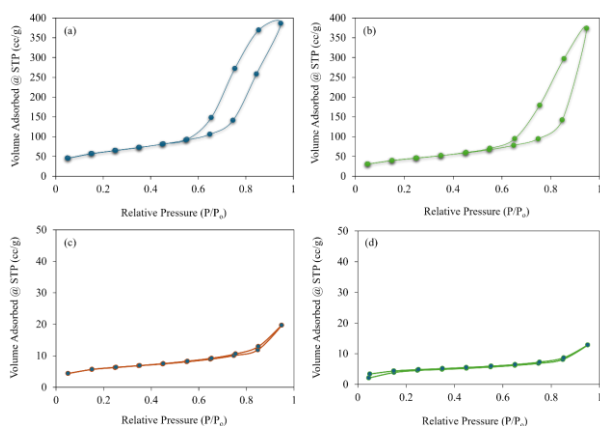


Figure 5. Isothermal graph of a) SCG, b) SSCGNK, c) SSCGK550, and d) SSCGK700

Table 2. GSA results of mesoporous silica synthesized

Sample	Surface Area (m ² /g)	Pore Size (nm)	Pore Volume (cc/g)
SCG	209.291	5.73	0.599
SSCGNK	150.613	7.70	0.580
SSCGK550	19.633	3.11	0.031
SSCGK700	14.974	2.66	0.020

In contrast, SSCGK550 and SSCGK700 display less distinct hysteresis loops and adsorption curves that tend to flatten at higher relative pressures. Similar results were reported by Saikumari *et al.* [14], this behavior resembles a transition toward Type III isotherms, which are typically associated with weaker adsorbent–adsorbate interactions and reduced monolayer formation. The change in isotherm shape suggests that high-temperature calcination may have altered the pore structure, possibly through partial pore shrinkage or structural rearrangement, leading to decreased mesoporosity and reduced surface accessibility.

Quantitative GSA data (Table 2) show that SCG possesses the highest surface area at 209.291 m²/g, with a pore size of 5.73 nm and a pore volume of 0.599 cc/g. Meanwhile, SSCGNK has a surface area of 150.613 m²/g with a larger pore size of 7.70 nm and a pore volume of 0.580 cc/g. After calcination, both the surface area and pore volume decreased drastically, reaching 19.663 m²/g and 0.031 cc/g for SSCGK550, and 14.974 m²/g and 0.020 cc/g for SSCGK700. The pore size also decreased to 3.11 nm and 2.66 nm, respectively. This phenomenon occurs because, during calcination, sintering of neighboring silica takes place, where adjacent particles fuse together, thereby reducing pore size [15]. Additionally, dehydroxylation and the removal of surfactants at high temperatures cause shrinking of the mesopore diameter and a reduction in pore volume [16].

The drastic reduction in textural parameters after calcination indicates that high-temperature treatment leads to the removal of cellulose organic components and the degradation of the pore structure, which in turn decreases the adsorption capacity of the material. The

SSCGNK exhibits mesoporous characteristics that remain relatively good, although more heterogeneous compared to SCG. Based on the pore size distribution curves, SCG displays a sharp distribution and relatively small pore size, indicating a more homogeneous structure. In contrast, the SSCGNK presents larger pore sizes with a broader distribution, reflecting a lower degree of structural homogeneity.

Overall, the GSA results indicate that pore structure and surface area are strongly influenced by the calcination treatment [14]. The incorporation of cellulose contributes to the formation of a denser structure, whereas the calcination process leads to pore narrowing or even pore collapse, which may affect the effectiveness of UAN fertilizer encapsulation and release in practical applications [11].

3.4.3. SEM-EDX

Scanning Electron Microscopy–Energy Dispersive X-ray (SEM–EDX) analysis was conducted to characterize the morphology and elemental composition of non-calcined cellulose–silica and cellulose–silica that had undergone calcination at different temperatures. The following images illustrate the morphology of the resulting samples. In Figure 6a, the morphology of the SSCGNK particles shows an irregular surface structure with randomly aggregated particles, indicating that the cellulose material has not fully decomposed. In Figure 6b, the morphology of the SSCGK550 exhibits more homogeneous particles, with granular forms that begin to agglomerate more uniformly compared to the non-calcined sample. In Figure 6c, the morphology of the SSCGK700 displays particles that appear more compact and smaller than those in the previous two samples. As the calcination temperature increases, the particle size and morphology decrease and become more compact. This is attributed to the degradation of cellulose at high temperatures, which causes the organic material to evaporate, leaving only the silica phase. Consequently, the pore structure undergoes shrinkage, resulting in a material with lower porosity

Based on SEM–EDX analysis (Table 3), SSCGNK contains 31.84% C, 9.05% N, 51.41% O, 7.50% Si, and trace amounts of P and K (0.01%). After calcination at 550°C, the carbon content decreases to 28.83% and nitrogen to 3.21%, while oxygen increases to 56.71% and silicon to 10.52%. In SSCGK700, carbon further decreases to 18.33%, nitrogen to 4.03%, oxygen increases to 58.42%, and silicon rises significantly to 17.94%, with slight increases in P and K (0.02%).

The presence of C, N, O, and Si confirms the coexistence of organic components (cellulose, glutaraldehyde, and UAN fertilizer) and the inorganic silica framework within the composites. The relatively high carbon content in SSCGNK indicates that organic constituents remain dominant prior to thermal treatment. The higher nitrogen content in the SSCGNK sample suggests that nitrogen-containing species from UAN fertilizer are retained more effectively before calcination.

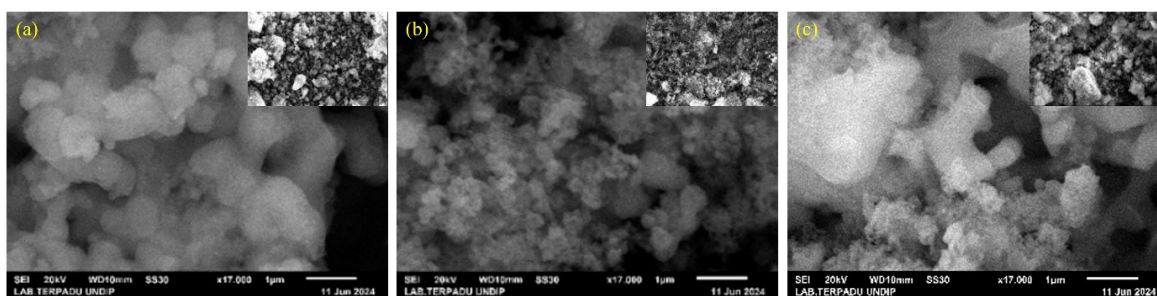


Figure 6. SEM-EDX images of a) SSCGNK, b) SSCGK 550, c) SSCGK700 at 17,000× magnification

Table 3. Surface elemental composition of silica composites determined by SEM-EDX

Sample	C (wt%)	N (wt%)	O (wt%)	Si (wt%)	P (wt%)	K (wt%)
SSCGNK	31.84	9.05	51.41	7.50	0.01	0.01
SSCGK550	28.83	3.21	56.71	10.52	0.01	0.01
SSCGK700	18.33	4.03	58.42	17.94	0.02	0.02

The progressive decrease in carbon content with increasing calcination temperature indicates thermal degradation of cellulose and other organic components. The reduction in nitrogen content is likely associated with partial decomposition or volatilization of nitrogen-containing species during heating, rather than solely reduced adsorption capacity. Concurrently, the increase in silicon and oxygen percentages reflects the relative enrichment of the inorganic SiO₂ framework as organic fractions are removed. It should be noted that EDX analysis represents surface elemental composition and does not fully describe the distribution of elements within internal pores. Therefore, conclusions regarding fertilizer loading and pore distribution require complementary characterization techniques.

3.4.4. Pot Experiment

Based on observations of plant height, the combination of liquid organic fertilizer types and concentrations did not produce statistically significant differences among treatments. This result may indicate that the nutrient supply from the applied liquid fertilizers was insufficient to markedly influence vegetative growth. Plant height in pakcoy during the vegetative phase is primarily governed by cell division, cell elongation, and early cell differentiation, processes that depend strongly on adequate nitrogen availability to support protein synthesis and protoplasm formation in apical tissues [17, 18].

In contrast, the pot experiment evaluating UAN SRF demonstrated a noticeable effect on plant performance. As shown in Table 4 and Figure 7, pakcoy treated with SSCGK550 exhibited superior growth compared to other treatments. Rapid growth was observed beginning on day 6, followed by vigorous leaf expansion until day 15. Significant differences in growth rate and biomass accumulation were observed among UAN fertilizer treatments, with SSCGK550 showing the best overall performance.

The improved growth under SSCGK550 treatment may be attributed to structural modifications induced by calcination. Calcination at 550°C likely enhanced pore development and surface accessibility, enabling more controlled nutrient release from the silica matrix. This controlled-release behavior may have ensured a more sustained nitrogen supply during the vegetative stage, thereby supporting continuous growth. In contrast, higher calcination temperature (700°C) may have reduced organic content and altered pore structure, potentially affecting nutrient retention capacity.

3.4.5. Plant Height

The observational data and mean comparison analysis using Duncan’s Multiple Range Test (DMRT) for the 0–15 day period are presented in Table 5. Although the EDX results (Table 3) indicate that SSCGK550 has lower surface nitrogen (N) than other samples, the growth experiment shows that SSCGK550 produced the highest plant height and leaf number in pakcoy. This finding suggests that total surface nitrogen content does not directly determine nutrient effectiveness or plant uptake efficiency.

Calcination at 550°C likely optimized the mesoporous silica structure by enhancing pore uniformity and removing residual organic matter that may have obstructed pore channels. The resulting structural improvement facilitates more controlled diffusion and gradual nutrient release [19]. In contrast, higher nitrogen percentages detected by EDX may reflect surface accumulation rather than bioavailable nitrogen. Since EDX measures only surface elemental composition, it does not fully represent nitrogen distribution within internal pores or the bulk matrix. Silviana *et al.* [20] reported that lower nitrogen content detected by EDX does not necessarily indicate reduced active nitrogen availability. Similarly, Azmiyawati *et al.* [11] observed that silica calcined at moderate temperatures exhibited adsorption-desorption characteristics consistent with controlled nutrient release behavior. The release profile shown in Figure 7 further supports this explanation, as SSCGK550 exhibits a gradual, sustained nutrient release pattern. Such controlled release provides a continuous, yet moderate, nitrogen supply, which is more favorable for vegetative growth than rapid nutrient leaching. This mechanism likely explains the superior growth performance of pakcoy under the SSCGK550 treatment.

Table 4. Plant height of pakcoy under different UAN fertilizer treatments

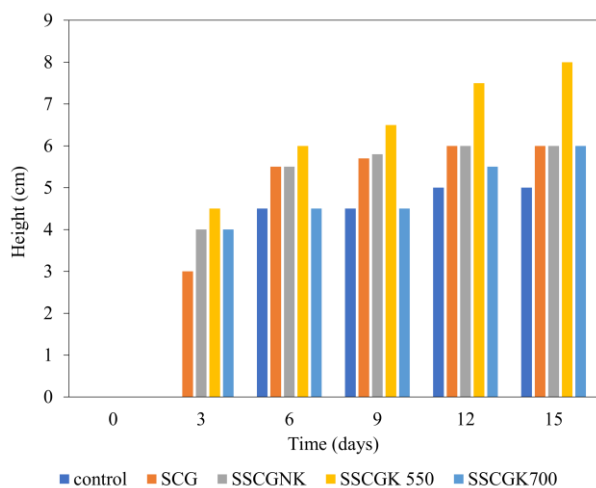
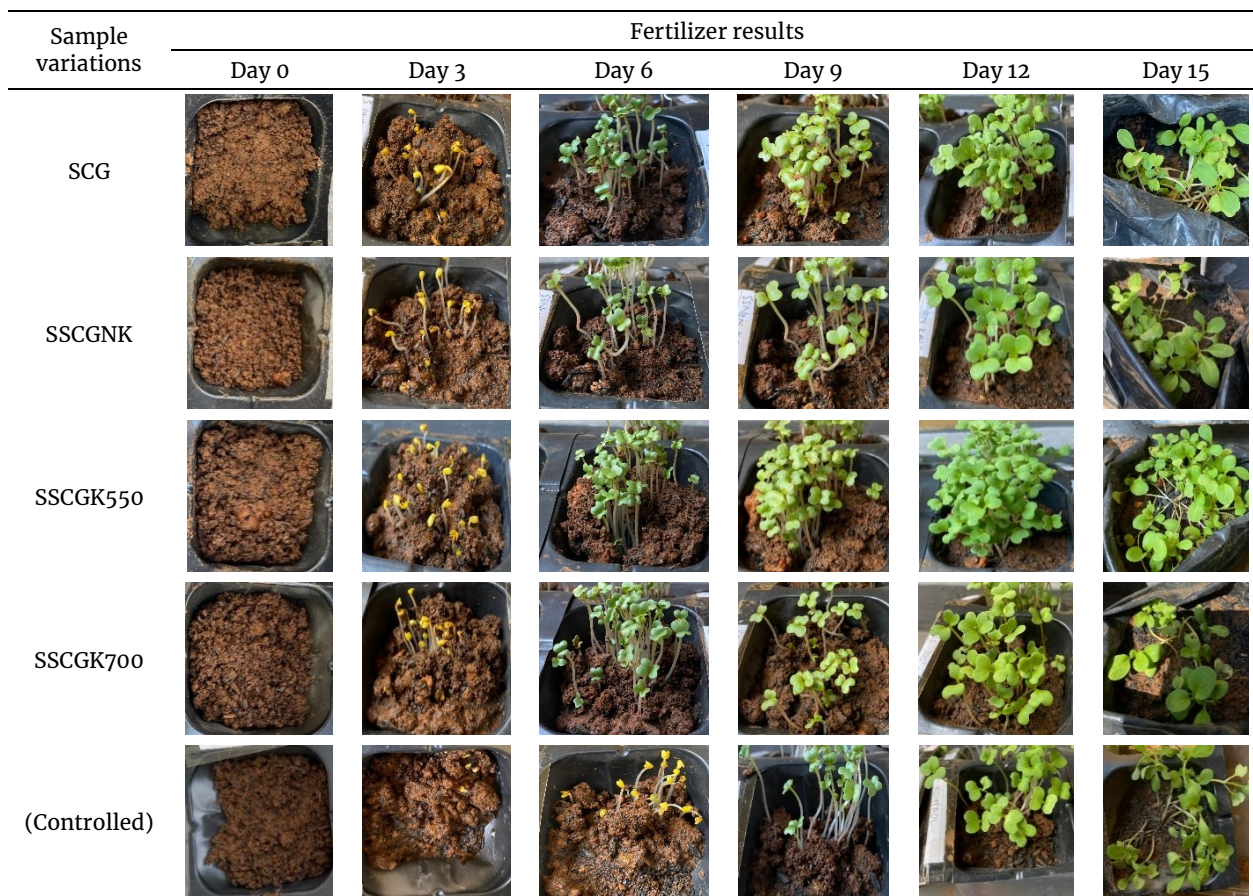


Figure 7. Plant height of pakcoy under different UAN fertilizer treatments

Table 5. Effect of UAN fertilizer calcination temperature on pakcoy plant height

Sample	Day 0	Day 3	Day 6	Day 9	Day 12	Day 15
SCG	-	3	5.5	5.7	6	6
SSCGNK	-	4	5.5	5.8	6	6
SSCGK550	-	4.5	6	6.5	7.5	8
SSCGK700	-	4	4.5	4.5	5.5	6
Controlled	-	0.5	4.5	4.5	5	5

Values represent mean plant height (cm) during 15 days of observation.

Table 6. Effect of UAN fertilizer calcination temperature on the number of pakcoy leaves

Sample	Day 0	Day 3	Day 6	Day 9	Day 12	Day 15
SCG	-	-	2	2	2	6
SSCGNK	-	-	2	2	2	6
SSCGK550	-	-	2	2	4	8
SSCGK700	-	-	2	2	2	4
Controlled	-	-	-	2	2	3

3.4.6. Number of Leaves

The observational data and the results of DMRT for the 0–15 day period are presented in Table 6. Observations of leaf development over 15 days demonstrate clear differences among UAN fertilizer treatments. The SSCGK550 sample produced the highest number of leaves, reaching eight leaves on day 15. This superior performance suggests that calcination at 550°C enhances fertilizer effectiveness, likely by promoting a controlled, sustained nutrient-release pattern. A gradual nitrogen supply is particularly important for leaf formation, as nitrogen plays a central role in chlorophyll synthesis and vegetative growth.

In contrast, SSCGK700 produced only four leaves, indicating reduced effectiveness compared to SSCGK550. Excessively high calcination temperatures may alter pore structure and reduce nutrient retention capacity, potentially affecting the release profile required for optimal plant growth [15]. Overall, the results indicate

that moderate calcination temperature (550°C) provides a more favorable balance between structural stability and nutrient-release performance, leading to improved vegetative development in pakcoy.

3.4.7. Fertilizer Release Test

Based on UV–Vis absorbance measurements and calculated nitrate concentrations, the nitrate release profile of UAN fertilizer is presented in Figure 8. The results demonstrate that calcination temperature significantly influences both the rate and total amount of nutrient release. All samples show an increasing nitrate concentration over time; however, the magnitude of release differs markedly among treatments.

The SCG sample exhibited gradual nutrient release, reaching 424 ppm on day 10. In comparison, SSCGNK showed a higher release, reaching 641.6 ppm over the same period. The presence of organic components in the non-calcined sample may enhance water penetration and facilitate faster diffusion of nitrate from the matrix.

Calcination at 550°C (SSCGK550) produced the highest nitrate release, reaching 893.7 ppm on day 10. This suggests that moderate-temperature calcination optimizes pore accessibility and structural uniformity, thereby enhancing nutrient diffusion from the silica matrix into the surrounding medium. Improved mesoporosity likely facilitates a more effective balance between nutrient retention and controlled release.

In contrast, calcination at 700°C significantly reduced nutrient release, with a final concentration of only 77.2 ppm. Excessive thermal treatment may lead to pore shrinkage, structural densification, or partial loss of active adsorption sites, limiting nutrient diffusion [15]. Consequently, the material's release capacity becomes substantially restricted. Overall, these findings indicate that moderate calcination (550°C) provides the most favorable structural conditions for controlled yet effective nitrate release, which is consistent with the superior plant growth performance observed in the pot experiment.

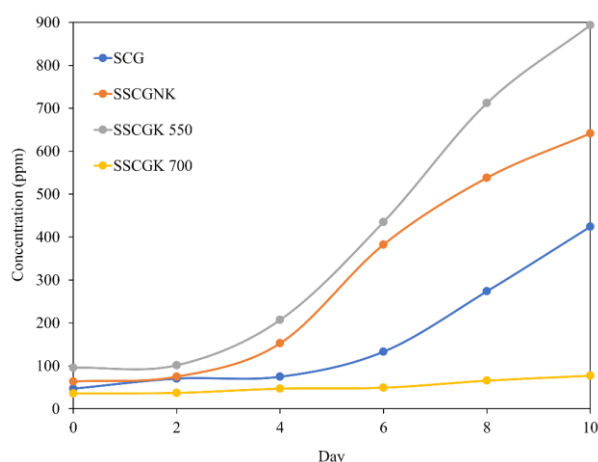


Figure 8. Slow-release graph of UAN fertilizer concentration variations

4. Conclusion

Mesoporous silica–cellulose composites subjected to calcination at 550 °C or 700 °C, followed by glutaraldehyde crosslinking, were successfully synthesized for UAN fertilizer encapsulation. FTIR analysis confirmed the presence of silanol (Si–OH), siloxane (Si–O–Si), and cellulose-derived functional groups, indicating successful integration of organic and inorganic components. SEM and textural analyses showed that calcination significantly influenced pore structure and surface morphology. Among the tested materials, the composite calcined at 550°C (SSCGK550) showed the best performance. This sample exhibited optimized structural characteristics that promoted effective nutrient retention and controlled nitrate release. The improved release behavior was directly reflected in the pot experiment, where SSCGK550 produced the highest plant height (8 cm) and leaf number (8 leaves) within 15 days. Overall, moderate-temperature calcination (550°C) provided the optimal balance between structural stability and nutrient-release efficiency, highlighting the strong potential of this silica–cellulose composite as a nitrogen–based slow-release fertilizer carrier.

References

- [1] Manxian Zhang, Jisheng Yang, Preparation and characterization of multifunctional slow release fertilizer coated with cellulose derivatives, *International Journal of Polymeric Materials and Polymeric Biomaterials*, 70, 11, (2021), 774–781 <https://doi.org/10.1080/00914037.2020.1765352>
- [2] David D. Myrold, 15 - Transformations of nitrogen, in: T.J. Gentry, J.J. Fuhrmann, D.A. Zuberer (Eds.) *Principles and Applications of Soil Microbiology (Third Edition)*, Elsevier, 2021, <https://doi.org/10.1016/B978-0-12-820202-9.00015-0>
- [3] T. Rütting, H. Aronsson, S. Delin, Efficient use of nitrogen in agriculture, *Nutrient Cycling in Agroecosystems*, 110, 1, (2018), 1–5 <https://doi.org/10.1007/s10705-017-9900-8>
- [4] Valensi Kautsar, Mawandha Hangger Gahara, Bimantara Aldymas, Respon bibit kelapa sawit terhadap aplikasi urea berlapis zeolit sebagai pupuk slow release nitrogen, *Jurnal Pengelolaan Perkebunan*, 4, 1, (2023), 1–7 <https://doi.org/10.54387/jpp.v4i1.32>
- [5] Priya E., Sudipta Sarkar, Pradip K. Maji, A review on slow-release fertilizer: Nutrient release mechanism and agricultural sustainability, *Journal of Environmental Chemical Engineering*, 12, 4, (2024), 113211 <https://doi.org/10.1016/j.jece.2024.113211>
- [6] Saulo Augusto Quassi de Castro, Thomas Kichey, Daniel Pergament Persson, Jan Kofod Schjoerring, Leaf Scorching following Foliar Fertilization of Wheat with Urea or Urea–Ammonium Nitrate Is Caused by Ammonium Toxicity, *Agronomy*, 12, 6, (2022), 1405 <https://doi.org/10.3390/agronomy12061405>
- [7] José Arnaldo S. Costa, Roberta A. de Jesus, Danilo O. Santos, Jordan B. Neris, Renan T. Figueiredo, Caio M. Paranhos, Synthesis, functionalization, and

- environmental application of silica-based mesoporous materials of the M41S and SBA-n families: A review, *Journal of Environmental Chemical Engineering*, 9, 3, (2021), 105259 <https://doi.org/10.1016/j.jece.2021.105259>
- [8] Hongwei Zhang, Hongxu Liang, Libin Xing, Wei Ding, Zengchao Geng, Chenyang Xu, Cellulose-based slow-release nitrogen fertilizers: Synthesis, properties, and effects on pakchoi growth, *International Journal of Biological Macromolecules*, 244, (2023), 125413 <https://doi.org/10.1016/j.ijbiomac.2023.125413>
- [9] Dhyna Analyses Trirahayu, Ridwan P. Putra, Achmad Syarif Hidayat, Muhammad Iqbal Perdana, Erwina Safitri, Synthesis and performance evaluation of cellulose-based slow-release fertilizer: a review, *KOVALEN: Jurnal Riset Kimia*, 8, 1, (2022), 1-16 <https://doi.org/10.22487/kovalen.2022.v8.1.15731>
- [10] Gita Citra Santi, Maya Rahmayanti, Effect of Solution pH to Indigosol Blue Adsorption on Humic Acid Isolated from Kalimantan Peat Oil, *Proceeding International Conference on Science and Engineering*, 2, (2019), 193-195 <https://doi.org/10.14421/icse.v2.84>
- [11] Choiril Azmiyawati, Ari Setyorini, Hasan Muhtar, Sriatun Sriatun, Adi Darmawan, Optimizing nitrogen delivery: Controlled release of fertilizer using mesoporous silica for sustainable agriculture, *Particulate Science and Technology*, 43, 4, (2025), 592-602 <https://doi.org/10.1080/02726351.2025.2478222>
- [12] Tetyana M. Budnyak, Ievgen V. Pylypchuk, Valentin A. Tertykh, Elina S. Yanovska, Dorota Kolodynska, Synthesis and adsorption properties of chitosan-silica nanocomposite prepared by sol-gel method, *Nanoscale Research Letters*, 10, 1, (2015), 87 <https://doi.org/10.1186/s11671-014-0722-1>
- [13] Edwin Makhado, Preparation of carboxymethyl cellulose-based silica hydrogel nanocomposite for methylene blue and malachite green dyes adsorption from aqueous solution, *Surfaces and Interfaces*, 56, (2025), 105699 <https://doi.org/10.1016/j.surfin.2024.105699>
- [14] N. Saikumari, S. Monish Dev, S. Avinaash Dev, Effect of calcination temperature on the properties and applications of bio extract mediated titania nano particles, *Scientific Reports*, 11, 1, (2021), 1734 <https://doi.org/10.1038/s41598-021-80997-z>
- [15] Julia C. Steinbach, Fabio Fait, Hermann A. Mayer, Andreas Kandelbauer, Sol-Gel-Controlled Size and Morphology of Mesoporous Silica Microspheres Using Hard Templates, *ACS Omega*, 8, 33, (2023), 30273-30284 <https://doi.org/10.1021/acsomega.3c03098>
- [16] Zhong-Xi Sun, Ting-Ting Zheng, Qi-Bing Bo, Miao Du, Willis Forsling, Effects of calcination temperature on the pore size and wall crystalline structure of mesoporous alumina, *Journal of Colloid and Interface Science*, 319, 1, (2008), 247-251 <https://doi.org/10.1016/j.jcis.2007.11.023>
- [17] M. Idris, Sutarno, B. Rusdiarso, Composite of amorphous silica encapsulated urea as a slow-release fertilizer, *IOP Conference Series: Materials Science and Engineering*, 1053, (2021), 012003 <https://doi.org/10.1088/1757-899X/1053/1/012003>
- [18] Muchammad Joko Mustofa, Andriani Eko Prihatiningrum, Intan Rohma Nurmallasari, Effect of Types and Concentration of Liquid Organic Fertilizer on the Growth and Production of Pakcoy Plants (*Brassica Rapa L.*), *IOP Conference Series: Earth and Environmental Science*, 1104, 1, (2022), 012010 <https://doi.org/10.1088/1755-1315/1104/1/012010>
- [19] Adriano M. Basso, Bruna P. Nicola, Katia Bernardo-Gusmão, Sibebe B. C. Pergher, Tunable Effect of the Calcination of the Silanol Groups of KIT-6 and SBA-15 Mesoporous Materials, *Applied Sciences*, 10, 3, (2020), 970 <https://doi.org/10.3390/app10030970>
- [20] S. Silviana, Atikah Ayu Janitra, Erwin Ade Pratama Pangihutan Sagala, Silvie Elmia Sari, Afriza Ni'matus Sa'adah, Febio Dalanta, Modification of mesoporous silica using 3-aminopropyltriethoxysilane as slow-release urea fertilizer, *AIP Conference Proceedings*, 2689, 3, (2023), 060007 <https://doi.org/10.1063/5.0114910>